



Quasi 3D ECE imaging system for study of MHD instabilities in KSTARa)

G. S. Yun, W. Lee, M. J. Choi, J. Lee, M. Kim, J. Leem, Y. Nam, G. H. Choe, H. K. Park, H. Park, D. S. Woo, K. W. Kim, C. W. Domier, N. C. Luhmann Jr., N. Ito, A. Mase, and S. G. Lee

Citation: [Review of Scientific Instruments](#) **85**, 11D820 (2014); doi: 10.1063/1.4890401

View online: <http://dx.doi.org/10.1063/1.4890401>

View Table of Contents: <http://scitation.aip.org/content/aip/journal/rsi/85/11?ver=pdfcov>

Published by the [AIP Publishing](#)

Articles you may be interested in

[Alternative optical concept for electron cyclotron emission imaginga\)](#)

Rev. Sci. Instrum. **85**, 11D802 (2014); 10.1063/1.4884902

[Measurements of the deuterium ion toroidal rotation in the DIII-D tokamak and comparison to neoclassical theorya\)](#)

Phys. Plasmas **19**, 056107 (2012); 10.1063/1.3694656

[Measurement and modeling of three-dimensional equilibria in DIII-Da\)](#)

Phys. Plasmas **18**, 056121 (2011); 10.1063/1.3593009

[Development of KSTAR ECE imaging system for measurement of temperature fluctuations and edge density fluctuationsa\)](#)

Rev. Sci. Instrum. **81**, 10D930 (2010); 10.1063/1.3483209

[Coupling of global toroidal Alfvén eigenmodes and reversed shear Alfvén eigenmodes in DIII-Da\)](#)

Phys. Plasmas **14**, 056102 (2007); 10.1063/1.2436489

Nor-Cal Products



Manufacturers of High Vacuum
Components Since 1962

- Chambers
- Motion Transfer
- Flanges & Fittings
- Viewports
- Foreline Traps
- Feedthroughs
- Valves



www.n-c.com
800-824-4166

Quasi 3D ECE imaging system for study of MHD instabilities in KSTAR^{a)}

G. S. Yun,^{1,b)} W. Lee,² M. J. Choi,¹ J. Lee,¹ M. Kim,¹ J. Leem,¹ Y. Nam,¹
 G. H. Choe,¹ H. K. Park,² H. Park,³ D. S. Woo,³ K. W. Kim,³ C. W. Domier,⁴
 N. C. Luhmann, Jr.,⁴ N. Ito,⁵ A. Mase,⁶ and S. G. Lee⁷

¹Department of Physics, Pohang University of Science and Technology, Pohang 790-784, Korea

²Ulsan National Institute of Science and Technology, Ulsan 689-798, Korea

³School of Electrical Engineering, Kyungpook National University, Daegu 702-701, Korea

⁴Department of Electrical and Computer Engineering, University of California, Davis, California 95616, USA

⁵KASTEK, Kyushu University, Kasuga-shi, Fukuoka 812-8581, Japan

⁶Ube National College of Technology, Ube-shi, Yamaguchi 755-8555, Japan

⁷National Fusion Research Institute, Daejeon 305-333, Korea

(Presented 3 June 2014; received 7 June 2014; accepted 3 July 2014; published online 22 July 2014)

A second electron cyclotron emission imaging (ECEI) system has been installed on the KSTAR tokamak, toroidally separated by 1/16th of the torus from the first ECEI system. For the first time, the dynamical evolutions of MHD instabilities from the plasma core to the edge have been visualized in quasi-3D for a wide range of the KSTAR operation ($B_0 = 1.7\sim 3.5$ T). This flexible diagnostic capability has been realized by substantial improvements in large-aperture quasi-optical microwave components including the development of broad-band polarization rotators for imaging of the fundamental ordinary ECE as well as the usual 2nd harmonic extraordinary ECE. © 2014 AIP Publishing LLC. [<http://dx.doi.org/10.1063/1.4890401>]

I. INTRODUCTION

Fast 2D imaging diagnostic systems for electron temperature (T_e) fluctuations in high temperature magnetized plasmas have been realized recently or are being developed on many tokamaks¹⁻⁷ by extending microwave technologies used in the conventional 1D electron cyclotron emission (ECE) radiometry into 2D. The ECE imaging (ECEI) systems have enabled direct visualization of a variety of magneto-hydrodynamic (MHD) instability structures in the poloidal cross-section of the tokamak plasma with fine spatial and time resolutions.⁸⁻¹³ Local and nonlinear dynamics immanent in MHD instabilities such as sawteeth,^{8,12} tearing modes,⁹ Alfvén eigenmodes,¹⁰ and edge localized modes¹¹ have been revealed, which were unresolvable using conventional 1D profile diagnostics or 2D tomography. Comparisons with numerical simulations are now being actively pursued to understand the fine features in MHD instability structure and dynamics.

II. ECEI SYSTEMS ON THE KSTAR

The first ECEI system installed on the KSTAR tokamak⁴ has two independent arrays of detectors and a flexible microwave optics capable of simultaneous imaging of low-field side (LFS) and high-field side (HFS) in the same poloidal cross section (Fig. 1). Each detector box (see Fig. 5) contains a vertical array of 24 Schottky diode detectors optimized for the detection of the 2nd harmonic extraordinary

(X2) mode ECE emissions, which are approximately vertically polarized, in a broad frequency range, 80–140 GHz. The array box can also be used to detect the fundamental Ordinary (O1) mode ECE emissions, which are approximately horizontally polarized, using polarization rotators for discharges with high magnetic field (see Sec. III C). The Heterodyne mixing and subsequent intermediate frequency (IF: 2.5–9 GHz) electronics (not shown in the figure) provide 8 radial channels covering a rectangular field of view of height ~ 50 cm and width ~ 15 cm with spatial resolution ≤ 2 cm and time resolution $\leq 2 \mu\text{s}$. Following the optical axis from the plasma, the ECEI system consists of zoom optics, beam splitter, focal lenses, planar notch filters, dichroic high-pass filter plates (Fig. 3), and detector array boxes (Fig. 5).

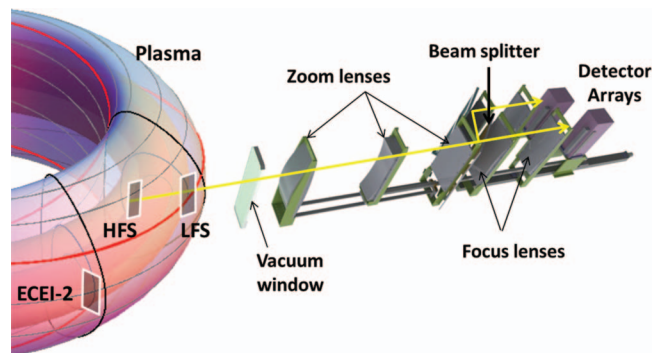


FIG. 1. Schematic of the ECEI system on the KSTAR tokamak. Rectangular regions indicated by HFS and LFS are the two fields of view of the 1st ECEI system and the other is the field of view of the 2nd ECEI system. Along the two optical axes of the 1st system indicated by the straight lines (yellow), shown are optical lenses, beam splitter, and array boxes. Other microwave optical components are explained in subsequent figures.

^{a)}Contributed paper, published as part of the Proceedings of the 20th Topical Conference on High-Temperature Plasma Diagnostics, Atlanta, Georgia, USA, June 2014.

^{b)}Author to whom correspondence should be addressed. Electronic mail: gusun@postech.ac.kr

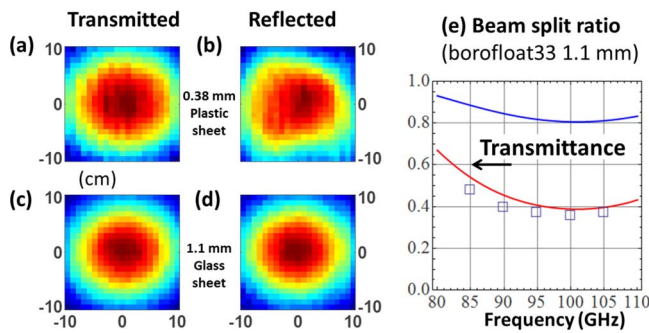


FIG. 2. Transmitted and reflected beam power profiles for the thin plastic sheet ((a) and (b), respectively) and for the thin borofloat33 glass sheet ((c) and (d), respectively). All measurements were done using 90 GHz Gaussian beam. (e) Beam split ratio of the 45° tilt glass sheet. Squares are measurements and the red (lower) solid curve is the calculated transmission coefficient for s-polarized waves. The blue (upper) solid curve is for p-polarized waves.

After the successful operation of the dual-array ECEI system, another ECEI system with a single array has been installed to enable quasi 3D imaging of T_e fluctuations on the KSTAR. This system is combined with a microwave imaging reflectometry (MIR) system¹⁴ for simultaneous measurements of electron density (n_e) and temperature fluctuations. The two ECEI systems are toroidally separated by 1/16th of the torus (approximately 70 cm at the center and 90 cm in the LFS edge of the plasma), which is suitable for the study of 3D structure and toroidal inhomogeneity of MHD instabilities. The measurement of 3D turbulent structures is also envisioned.

In addition to adding the 3D imaging capability, substantial improvements have been made in many quasi-optical microwave components including the beam splitter, dichroic plates, and half-wave plates in order to improve the signal quality as well as to achieve a diagnostic flexibility for a wide operation range of the KSTAR toroidal field ($B_0 = 1.7\text{--}3.5$ T). Section III gives a short description on each of these microwave components as well as re-enforcement of electromagnetic shielding of the array box to reduce the external noise pickup. Note that the notch filters¹⁵ are not discussed in this paper although they are essential components for protection of the detector diodes from stray high-power microwaves because of on-going tests to resolve the dependence of the

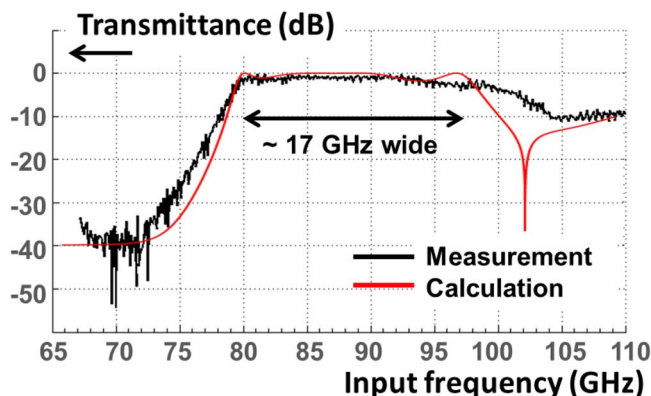


FIG. 3. Transmittance of a dichroic plate with the cutoff at 80 GHz. The pass band is ~ 17 GHz wide.

notch frequency, depth, and symmetry on the incident angle and beam profile. Finally, examples of 3D ECEI images are presented in the Conclusion to demonstrate the capability of the KSTAR ECEI system.

III. LARGE-APERTURE MICROWAVE COMPONENTS

A. Distortion-free beam splitter

The previous beam splitter was a large thin sheet of high-k dielectric plastic (Taconic RF35A2, thickness = 0.38 mm, dielectric constant = 3.5), which was prone to surface warping leading to distortion in the reflected beam (Fig. 2(b)). This problem has been solved by replacing the plastic beam splitter by a thin tempered glass sheet (borofloat33, thickness = 1.1 mm, dielectric constant = 4.6, size = 400 × 840 mm), a material commonly used for large flat panel displays. The glass sheet provides approximately 50:50 split ratios for a wide frequency range (Fig. 2(e)). The glass-based beam splitter also turned out to be a critical component in the MIR system where distortions in the probing and reflected beams could be detrimental.¹⁴

B. High-pass filters (dichroic plates)

Metallic plates with periodic holes called dichroic plates¹⁶ are commonly used to high-pass filter the radiation from the plasma for single-sided heterodyne mixing inside the detector array box. A complete set of dichroic plates with cutoff frequencies ranging from 75 GHz to 130 GHz have been fabricated to cover a broad range of the ECEI operation. The measured cutoff frequency, pass band, and insertion loss are in good agreement with the design (Fig. 3). The exception is the absence of resonant absorption expected from the theoretical model.¹⁶

C. Broad-band polarization rotators

For high magnetic field operation ($B_0 > 2.5$ T), the frequency of the X2 mode waves in the HFS becomes too large

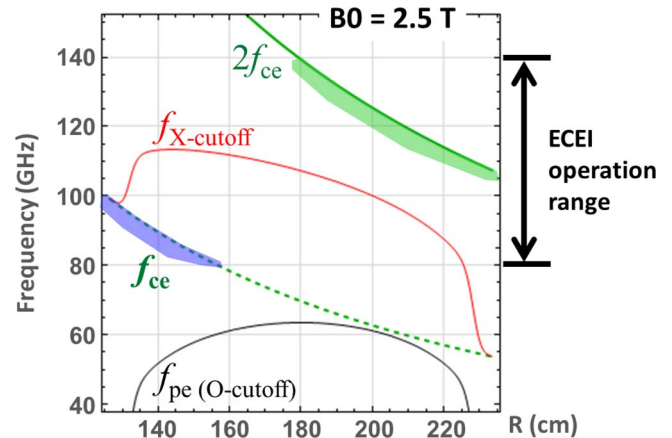


FIG. 4. ECE frequencies (f_{ce} , $2f_{ce}$) and cutoff frequencies (f_{pe} , $f_{X-cutoff}$) for typical KSTAR plasma with $B_0 = 2.5$ T. The shaded zones represent the radial coverage of the ECEI system within the operation frequency range. The HFS can be accessed by measurement of O1 mode emissions, whose frequency is well above the O-mode cutoff (f_{pe}).

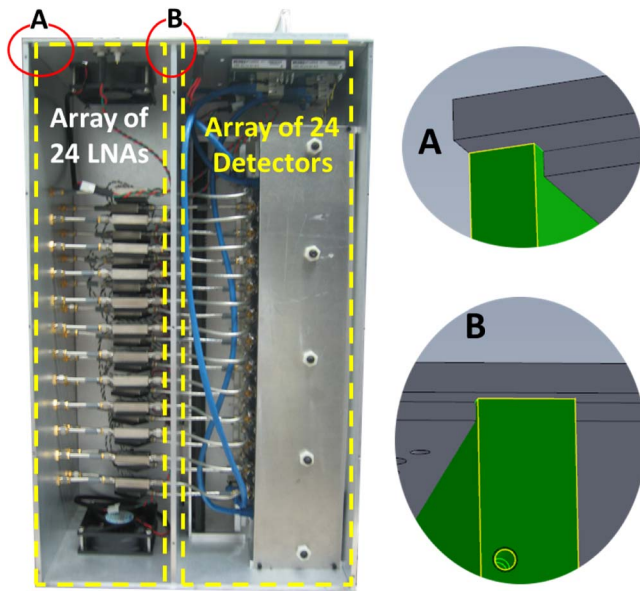


FIG. 5. New array box enclosure with separate compartments for LNAs (left side) and array detectors (right side). The two are connected by semi-rigid SMA cables through small holes. Close-up views A and B show the recessed seam structure between enclosure panels for minimization of radiation leakage.

for the ECEI arrays (Fig. 4). In order to access the HFS by measuring the O1 mode emission (vertically polarized) instead of the X2 mode emission (horizontally polarized) using the same array boxes, large-aperture polarization rotators have been developed by fabricating a simple groove pattern on high-density polyethylene (HDPE) plastic plate.¹⁷ The flexibility of selecting X2 or O1 mode greatly enhanced the diagnostic capability of the ECEI systems and contributed to the design of an ECEI system for ITER-like plasmas.¹⁸

D. Re-enforcement of the array box shield

Ambient electromagnetic sources in the IF range of the ECEI system are everywhere in the KSTAR experimental hall including wireless communication devices and the plasma discharge itself. In the old array box enclosure, ambient radiations were often leaked into the array detectors through the DC power cables, ventilation holes for the low-noise amplifiers (LNAs), and even through small seams between the enclosure panels. The leaked signals were subsequently amplified by LNAs, causing saturation or large spikes ($\sim 1V$) in the ECEI channels. In order to minimize the noise pickup by the array detectors, new array boxes have been built with enhanced shielding: electromagnetic separation of the array detectors from the LNAs using (Fig. 5(a)) and Lab tests showed ~ 40 dB reduction of external noise pickup in the ECEI IF range.

IV. CONCLUSION

The two ECEI systems at the KSTAR have been successfully operated for a wide range of KSTAR discharges thanks to these upgrades and improvements in the microwave opti-

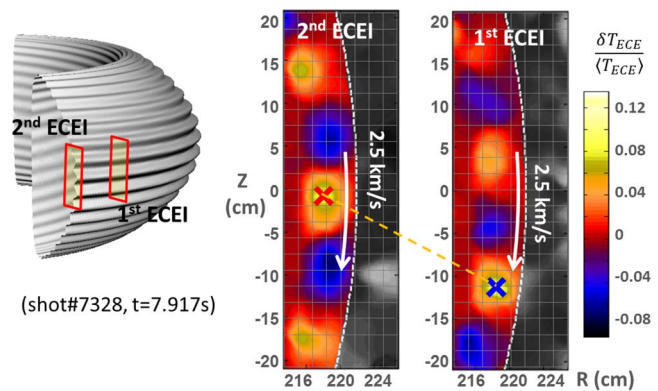


FIG. 6. Quasi 3D image of an edge-localized mode. The color scale is the normalized fluctuation amplitude of the emission temperature (T_{ECE}). The measured pitch ($\sim 6^\circ$) is identical within the uncertainty to the magnetic field line pitch estimated by equilibrium reconstruction.

cal components. Dynamical evolutions of MHD instabilities from the plasma core to the edge, such as internal kinks, tearing modes, and edge-localized modes, have been visualized in quasi 3D for the first time. An example of 3D imaging is demonstrated in Fig. 6, where the edge-localized mode formed along the magnetic field lines with the pitch angle $\sim 6^\circ$.¹⁹ Beyond the simple visualization of the spatial structure of MHD modes, the 3D imaging will enable studies on the helical inhomogeneity of MHD modes and the structure of turbulent fluctuations.

ACKNOWLEDGMENTS

We thank Mr. Yong-sun Kim and the KSTAR diagnostic team for their strong technical assistance. This work was supported by National Research Foundation of Korea under Grant No. NRF-2014M1A7A1A03029881 and BK21+ Advanced Nuclear Program, U.S. DOE under Contract No. DE-FG-02-99ER54531, and Japan-Korea Fusion Collaboration Program under Contract No. KHGJ-01.

- ¹H. Park *et al.*, *Rev. Sci. Instrum.* **75**, 3875 (2004).
- ²I. G. J. Classen *et al.*, *Rev. Sci. Instrum.* **81**, 10D929 (2010).
- ³B. Tobias *et al.*, *Rev. Sci. Instrum.* **81**, 10D928 (2010).
- ⁴G. S. Yun *et al.*, *Rev. Sci. Instrum.* **81**, 10D930 (2010).
- ⁵X. Ming *et al.*, *Plasma Sci. Technol.* **13**, 167 (2011).
- ⁶M. Jiang *et al.*, *Rev. Sci. Instrum.* **84**, 113501 (2013).
- ⁷Y. Nam *et al.*, *Rev. Sci. Instrum.* **83**, 10E318 (2012).
- ⁸H. K. Park *et al.*, *Phys. Rev. Lett.* **96**, 195003 (2006).
- ⁹I. G. J. Classen *et al.*, *Phys. Rev. Lett.* **98**, 035001 (2007).
- ¹⁰B. J. Tobias *et al.*, *Phys. Rev. Lett.* **106**, 075003 (2011).
- ¹¹G. S. Yun *et al.*, *Phys. Rev. Lett.* **107**, 045004 (2011).
- ¹²G. S. Yun *et al.*, *Phys. Rev. Lett.* **109**, 145003 (2012).
- ¹³M. J. Choi *et al.*, *Nucl. Fusion* **54**, 083010 (2014)
- ¹⁴W. Lee *et al.*, *J. Instrum.* **8**, C10018 (2013).
- ¹⁵Z. Shen *et al.*, *Plasma Fusion Res.* **2**, S1030 (2007).
- ¹⁶C. C. Chen, *IEEE Trans. Microwave Theory Tech.* **MTT-21**(1), 1 (1973).
- ¹⁷J. Lee, G. S. Yun, M. Kim, W. Lee, and H. K. Park, *J. Instrum.* **7**, C01037 (2012).
- ¹⁸W. Lee, G. S. Yun, Y. B. Nam, H. K. Park, and C. R. Seon, "Conceptual design of electron cyclotron emission imaging system for ITER-like high-temperature plasmas," *Plasma Phys. Controlled Fusion* (to be published).
- ¹⁹J. Lee *et al.*, *Rev. Sci. Instrum.* **85**, 063505 (2014).